Published OnlineFirst October 31, 2011; DOI: 10.1158/1078-0432.CCR-11-0166

Clinical Cancer Research

MicroRNA-494 Downregulates KIT and Inhibits Gastrointestinal Stromal Tumor Cell Proliferation

Won Kyu Kim, Misun Park, Young-Kook Kim, et al.

Clin Cancer Res 2011;17:7584-7594. Published OnlineFirst October 31, 2011.

Human Cancer Biology

Clinical Cancer Research

MicroRNA-494 Downregulates KIT and Inhibits Gastrointestinal Stromal Tumor Cell Proliferation

Won Kyu Kim[1,2], Misun Park[1,2], Young-Kook Kim[4], Kwon Tae You[4], Han-Kwang Yang[5], Jae Myun Lee[1,3], and Hoguen Kim[1,2]

Abstract

Purpose: Gain-of-function mutations and KIT overexpression are well-known tumorigenesis mechanisms in gastrointestinal stromal tumors (GIST). This study aimed to discover microRNAs (miRNA) that target KIT and reveal the relationship between the discovered miRNAs and KIT expression in GISTs.

Experimental Design: Fresh-frozen GISTs from 31 patients were used to confirm the relationship between miR-494 and KIT expression using quantitative reverse transcription-PCR to assess miR-494 expression levels and Western blotting to assess KIT protein expression levels. A luciferase assay was conducted for the target evaluation. The functional effects of miR-494 on GIST882 cells (GIST cell line with activating *KIT* mutation) were validated by a cell proliferation assay and fluoresce-activated cell sorting analysis.

Results: An inverse relationship was found between the expression levels of miR-494 and KIT in GISTs ($r = -0.490$, $P = 0.005$). The direct targeting of KIT by miR-494 was shown by the reduction in KIT expression after miR-494 overexpression and the increase in KIT expression after inhibiting endogenous miR-494 expression. We showed that miR-494 regulates KIT by binding two different seed match sites. Induced miR-494 overexpression in GIST882 reduced the expression of downstream molecules in KIT signaling transduction pathways, including phospho-AKT and phospho-STAT3. Finally, miR-494 overexpression provoked apoptosis and inhibited GIST cell growth, which were accompanied by changes in G_1 and S phase content.

Conclusion: Our findings indicate that miR-494 is a negative regulator of KIT in GISTs and overexpressing miR-494 in GISTs may be a promising approach to GIST treatment. *Clin Cancer Res; 17(24); 7584–94. ©2011 AACR.*

Introduction

The molecular genetics of gastrointestinal stromal tumors (GIST) are among the best understood of human tumors (1). Two oncogenes of the receptor tyrosine kinase family, *KIT* and *PDGFRA*, have gain-of-function mutations in approximately 70% and 15% of GISTs, respectively (2, 3). Mutations of these 2 genes cause sustained activation, resulting in constant stimulation of the downstream signaling pathways of KIT and platelet-derived growth factor receptor, alpha polypeptide (4, 5). Of these genes, KIT activation is especially crucial to the development and progression of GISTs (3). The downstream molecular pathways involved in GIST tumorigenesis after *KIT* mutation include PI3 kinase-AKT, Src family kinase, Ras-ERK, and JAK-STAT (6). Activation of these molecular pathways after KIT activation results in GIST tumorigenesis through cell proliferation activation and apoptotic signal inhibition (4, 6, 7).

The progression of GIST is successfully blocked by imatinib, which suppresses KIT by competitively binding its ATP-binding pocket, inhibiting KIT activation, and blocking the activation of the downstream MAP kinase and PI3 kinase-AKT pathways (7, 8). However, the development of imatinib resistance during imatinib treatment reduces the inhibitory effects of imatinib. Therefore, more diverse approaches to inhibit-activated KIT via posttranscriptional and posttranslational mechanisms are required for GISTs with KIT activation (9–11).

KIT overexpression has been reported as a characteristic feature of GISTs, and the presence of *KIT* mutations usually leads to strong KIT expression (12, 13). Although *KIT* mutations are present in approximately 70% of GISTs, KIT overexpression is observed in more than 90% of GISTs, suggesting that a complementary mechanism participates in KIT overexpression (2, 14). Dysregulation of microRNAs

Authors' Affiliations: [1]Brain Korea 21 Projects for Medical Science; Departments of [2]Pathology and [3]Microbiology, Yonsei University College of Medicine; [4]School of Biological Science and Center for National Creative Research; and [5]Department of Surgery, College of Medicine, Seoul National University, Seoul, Korea

Corresponding Author: Hoguen Kim, Department of Pathology, Yonsei University College of Medicine, Seoul 120752, Korea. Phone: 82-2-2228-1761; Fax: 82-2-363-5263; E-mail: hkyonsei@yuhs.ac

doi: 10.1158/1078-0432.CCR-11-0166

Translational Relevance

Gastrointestinal stromal tumors (GIST) have changed from being poorly defined to well-recognized tumors. Mutations of KIT and platelet-derived growth factor receptor, alpha polypeptide are major factors causing the development of GISTs. Of those genes, activating mutations of KIT are particularly crucial to the development and progression of GISTs. Imatinib (STI571), which blocks KIT activation, has been successfully applied to treat patients with GISTs. However, imatinib-resistant mutations are frequently found in patients with GISTs during treatment. Therefore, the development of alternative therapeutic tools is required. One of the alternatives is microRNA (miRNA)-based therapy. We previously found 5 miRNAs, the expression of which was inversely related to KIT expression in GISTs. Of these 5 miRNAs, we verified an inverse relationship between miR-494 and KIT expression in 31 GISTs. We also showed that miR-494 downregulates KIT, and miR-494 overexpression inhibits GIST cell growth. Therefore, KIT inactivation through miR-494 might be another promising approach for GIST treatment.

(miRNA) is a possible mechanism, as miRNAs play important roles in regulating gene expression in cancers (15, 16).

In erythroleukemic cells, miR-221/miR-222 are presently reported to target KIT (17). In GISTs, no miRNAs targeting KIT have been identified. We previously compared KIT expression and miRNA expression profiles in GISTs and identified 5 possible candidate miRNAs for which their expression is inversely related to KIT expression (13). In this study, we proposed that miR-494 regulates KIT expression by showing that (i) miR-494 expression is inversely correlated with KIT expression in GIST tissues, (ii) exogenous miR-494 induces KIT downregulation, and (iii) inhibition of endogenous miR-494 increases KIT expression. We also showed that miR-494 represses the proliferation of a GIST cell line with a KIT-activating mutation (GIST882; ref. 7). Taken together, our results suggest that miR-494 is involved in GIST tumorigenesis via regulating KIT expression.

Materials and Methods

Cell lines and culture

The GIST882 cell line with an activating KIT mutation (exon 13, K642E) was a generous gift from Dr. Jonathan Fletcher, Harvard University, Cambridge, MA. SNU216, SNU638, SNU1, NCI-N87, DLD-1, and HeLa cells were purchased from the Korean Cell Line Bank (Cancer Research Institute, Seoul, Korea). Cell culture images were taken with an IX71 camera (Olympus).

Patient and tissue samples

The 31 GISTs included in this study were identified in the Department of Pathology at Yonsei University Medical Center between August 1997 and June 2006 for molecular marker studies. Authorization to use these tissues for research purposes was obtained from the Institutional Review Board of Yonsei Medical Center. Some of the fresh specimens were obtained from the Liver Cancer Specimen Bank of the National Research Resource Bank Program of the Korea Science and Engineering Foundation of the Ministry of Science and Technology. Among the 31 GISTs, 17 samples had previously been used for miRNA profiling and proteomic analyses (12, 13, 18, 19). Conventional pathologic parameters including anatomic site, risk, and tumor size were examined prospectively without prior knowledge of the molecular data (Table 1). The GISTs were divided into 4 groups based on tumor risk according to the criteria of Fletcher and colleagues (1, 20).

RNA preparation and TaqMan miRNA assay

Total RNA was extracted from frozen tissues using TRIZOL (Life Technology). The expression levels of miRNA were quantified by the TaqMan miRNA assay (Applied Biosystems) and analyzed with an Applied Biosystems 7300 Real-Time PCR system. The assay ID was 002365 for miR-494 and 001093 for RNU6B, which was used to normalize miR-494 levels in the samples. Data analysis was conducted using both quantity values for miR-494 from GIST tissues and C_t values ($2^{-\Delta\Delta CT}$ method; ref. 21) to measure the induced expression of miR-494 in HeLa and GIST882 cells. All assays were carried out in triplicate.

Quantitative reverse transcription-PCR

The quantitative reverse transcription-PCR (qRT-PCR) primer sequences for KIT (PrimerBank ID; 4557695a2) and glyceraldehydes-3-phosphate dehydrogenase (GAPDH; PrimerBank ID; 2282013a2) were obtained from the PrimerBank database (http://pga.mgh.harvard.edu/primerbank/). The reaction was carried out in a final volume of 20 μL with Premix Ex Taq (TAKARA) according to the manufacturer's instructions. All reactions were run on an ABI Prism 7300 Real-Time PCR system in triplicate. The analysis of the results was conducted with quantity values using 7300 system SDS software (Applied Biosystems), and GAPDH was used for normalization. KIT mRNA levels were presented as the relative levels compared with the KIT mRNA levels in negative control samples in all figures.

miRNA mimics and transfection

Appropriate miRIDIAN miRNA mimics (nontargeting miRNA, miR-221, miR-222, and miR-494 miRNAs, and an miR-494 inhibitor; Thermo Scientific) were used in this study. All transfection experiments were carried out using Lipofectamine 2000 (Invitrogen). On the third day after transfection, all cells were harvested and managed for further Western blot analysis.

Western blots

Whole lysates from samples were prepared using passive lysis buffer (Promega). Primary antibodies used were against GAPDH (Trevigen), KIT, STAT3, ERK, phospho-ERK

Table 1. Clinicopathologic and genetic status of 31 GISTs

Case No.	Age/sex	Mutation status		Tumor				Cell type	Immunohistochemistry[a]	
		KIT	*PDGFR*	Size (cm)	Site	Mitotic count (/50HPF)	Risk		KIT	CD34
1	76/F	V560 del	Wild	8	Stomach	4	Intermediate	Spindle	+	+
2	56/F	V559A	Wild	5.5	Stomach	1	Intermediate	Spindle	+	+
3	64/F	D579 del	Wild	17	Stomach	20	High	Spindle	+	+
4	45/M	T574_R586 ins	Wild	10	Stomach	1	Intermediate	Spindle	+	+
5	68/F	V559D	Wild	8	Stomach	6	High	Spindle	+	+
6	58/M	Y553_Q556 del	Wild	6	Stomach	14	High	Spindle	+	+
7	58/M	V559D	Wild	16	Stomach	2	High	Mixed	+	+
8	74/F	D579 del	Wild	3	Stomach	4	Low	Spindle	+	+
9	51/M	W557R	Wild	3.5	Stomach	1	Low	Spindle	-	+
10	67/F	K550_Q556 del	Wild	9	Stomach	14	High	Mixed	+	+
11	43/F	W557R	Wild	9.8	Stomach	5	Intermediate	Spindle	+	+
12	42/F	L556_D569 ins	Wild	33	Stomach and spleen	4	High	Spindle	+	+
13	65/M	A504_Y505 ins	Wild	6.5	Abdominal cavity	23	High	Mixed	+	-
14	41/F	V559D	Wild	3.5	Stomach	5	Low	Spindle	+	+
15	49/F	V555_W557 del	Wild	13	Small bowel	15	High	Spindle	+	-
16	64/F	W557_K558 del	Wild	7.5	Stomach	10	High	Spindle	+	+
17	50/M	W557_K558 del	Wild	8	Stomach	23	High	Mixed	+	+
18	39/F	V559D	Wild	6.3	Stomach	8	High	Spindle	+	+
19	69/F	V559D	Wild	7	Stomach	2	Intermediate	Spindle	+	+
20	74/M	Q556_V559 del	Wild	6	Stomach	40	High	Mixed	+	+
21	46/F	M552_N572 del	Wild	5	Small bowel	74	High	Mixed	+	+
22	61/F	F509_F511 ins	Wild	5	Small bowel	0	Low	Mixed	+	-
23	79F	W557_K558 del	Wild	6.5	Small bowel	28	High	Spindle	+	+
24	64M	A504_Y505 ins	Wild	9.5	Small bowel	0	High	Spindle	+	+
25	47/M	A504_Y505 ins	Wild	9	Small bowel	20	High	Spindle	+	-
26	57/F	Wild	Wild	15	Stomach	1	High	Spindle	+	+
27	78/M	Wild	Wild	17	Stomach	49	High	Epithelioid	+	+
28	66/M	Wild	D842V	3	Stomach	0	Low	Mixed	-	-
29	44/F	Wild	Wild	1.3	Stomach	0	Very low	Spindle	+	+
30	38/F	Wild	Wild	5.5	Small bowl	0	High	Spindle	+	+
31	26/M	Wild	Wild	5.5	Stomach	4	Intermediate	Spindle	−	+

NOTE: [a]+ indicates that tumor cells express KIT. − indicates that tumor cells do not express KIT.

(Santa Cruz Biotechnology), phospho-KIT (Invitrogen), AKT, phospho-AKT, and phospho-STAT3 (Cell Signaling). The Western blot images were analyzed with a LAS-4000 Mini camera (Fujifilm).

Luciferase reporter assay

We designed a reporter assay by generating a vector (named N) with the coding sequences for *Renilla* luciferase and the entire 3′-untranslated region (UTR) sequences of KIT that were obtained from cDNAs of GIST882 cells. The 3′-UTR sequences (NCBI reference sequence; NM_000222) obtained from GIST882 by PCR amplification were cloned downstream of the SV40 enhancer and the early promoter-driven *Renilla* luciferase cassette in a pRL3 vector (Promega). The N vector was then used to generate 2 mutant constructs by mutating complementary seed sequences in the miR-494, miR-221, or miR-222–binding region. Using site-directed mutagenesis of the KIT 3′-UTR sequence in the N vector, both the M vector for miR-494, which had changes from nucleotides 1899 to 1902 (GTTT → CCGG), and the O vector for miR-221/miR-222, which had changes from nucleotides 1961 to 1964 (GTAG → CAGA), were generated. We also constructed 3 additional vectors from the M vector for the identification of additional miR-494–binding sites. Additional mutagenesis (GTTT → CCGG) of the potential miR-494–binding sites was conducted at positions 1,222 to 1,228 (TGTTTCT), 1,758 to 1,765 (GTGTTTCT), and 1,918 to 1,923 (ATGTTT). The vectors were named Ma, Mb, and Mc, respectively. The pGL3 luciferase reporter vector was used as a control vector for the dual luciferase assay (Promega). The oligonucleotide sequences used for vector construction are listed in Supplementary Table S1. Every dual luciferase assay was carried out by cotransfecting a control vector with the N, M, O, Ma, Mb, or Mc vector. All miRNA mimics were transfected at a concentration of 5 nmol/L. Two days after transfection, the luciferase activity was measured according to the manufacturer's instructions.

Cell proliferation assay

The GIST882 cells and DLD-1 cells were transfected with 50 nmol/L nontargeting miRNA or miR-494. The morphology of the 2 cells was examined daily and the cells were manually counted. The DLD-1 cells were washed with PBS and SCF containing media (10 ng/mL) with 2% FBS added to the cells after 48 hours of transfection. The numbers of the cells were counted 2 days after SCF stimulation. Every sample was duplicated, and the mean result was used for further analyses. A cell proliferation assay was independently conducted in triplicate.

Cell-cycle analysis

GIST882 cells were transfected with 50 nmol/L nontargeting miRNA or miR-494 in 60-mm dishes. On the 4th day after transfection, cells of each sample were stained in a solution of PBS, propidium iodine (PI; Abcam), and RNase A. All samples were analyzed by a FACS Calibur (BD Biosciences). We also analyzed apoptosis after miR-494 transfection in GIST882. For Annexin V staining, GIST882 cells were harvested on the 6th day after transfection of 50 nmol/L nontargeting miRNA or miR-494, and then a Fluorescein isothiocyanate Annexin V Apoptosis Detection Kit l (BD biosciences) was used according to the manufacturer's instructions. All samples were analyzed by a FACS Calibur. Each experiment was conducted in triplicate.

Results

Identifying miR-494 as a negative regulator of KIT

Our previous microarray data were used to evaluate the effect of 5 candidate miRNAs on KIT expression. Five candidate miRNAs were chosen because their expression levels had a statistically meaningful relationship with KIT expression in GISTs (13). To confirm the microarray data, 25 nmol/L of each of the 5 candidate miRNAs (miR-9, miR-142-5p, miR-370, miR-494, and miR-510) were transfected into KIT-overexpressing GIST882 cells. Western blot analysis of the transfected samples revealed that only miR-494 overexpression consistently reduced KIT protein expression (Supplementary Fig. S1). We validated the inverse correlation between miR-494 and KIT expression in GISTs by conducting qRT-PCR to measure miR-494 expression and Western blotting to assess KIT protein expression. For these analyses, we used 31 fresh-frozen GIST samples consisting of 25 GISTs with a *KIT* mutation and 6 GISTs without a *KIT* mutation (Table 1). The expression of miR-494 was analyzed using the mean values from 3 independent qRT-PCR experiments for each sample. The expression of KIT and miR-494 for each tissue was presented as a fold change (log scale) relative to the mean value of KIT and miR-494 expression, respectively, to compare the expression levels among the tumor samples (Fig. 1A and Supplementary Fig. S2). We found an inverse relationship between expression of KIT and miR-494 (Spearman's correlation coefficient, $r = -0.490$, $P = .005$).

After we validated the relationship between KIT and miR-494 expression in GISTs, we compared the efficiency of KIT downregulation of miR-494 with 2 previously reported KIT targeting miRNAs, miR-221/miR-222 (17). The ability of miR-494 to induce KIT downregulation was confirmed by transfecting GIST882 cells with 25 nmol/L nontargeting miRNA, miR-494, miR-221, or an miR-494 inhibitor. The nontargeting miRNA was used as a negative control, whereas miR-221 served as a positive control for comparisons with miR-494. The induction of miR-494 after transfection was determined by qRT-PCR. When we transfected GIST882 cells with 25 nmol/L miR-494, miR-494 expression was increased approximately 25-fold compared with that in nontransfected cells (Supplementary Fig. S3A). The results of Western blotting showed significant downregulation of KIT expression when the cells were transfected with miR-494 or miR-221, with miR-494 having greater efficacy than miR-221. qRT-PCR analysis revealed the same expression pattern as the Western blot analysis, except for slightly increased KIT mRNA levels in the cells transfected with an miR-494 inhibitor (Fig. 1B).

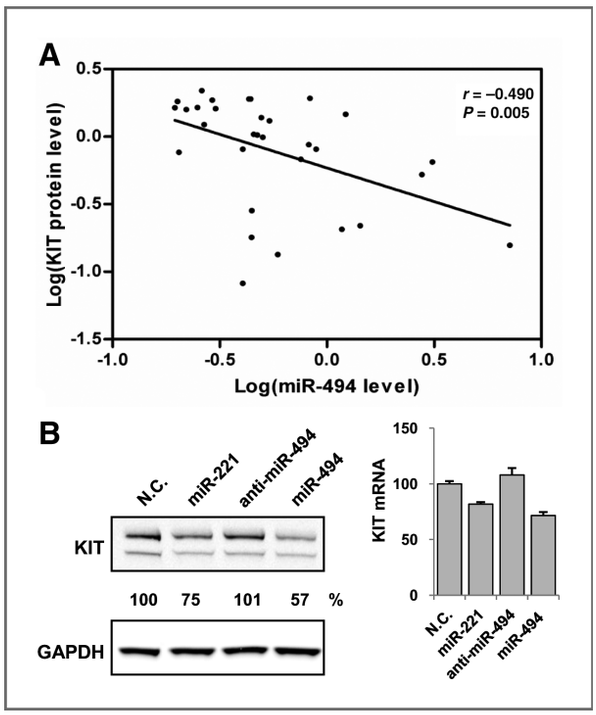

Figure 1. KIT expression is inhibited by miR-494 overexpression. A, KIT protein expression is inversely correlated with miR-494 expression. Western blotting and qRT-PCR was used to quantify the expression of KIT and miR-494, respectively. An inverse relationship between KIT protein expression and miR-494 expression was evident ($r = -0.490$, $P = .005$). B, changes in KIT protein expression after miR-494 transfection. GIST882 cells were transfected with 25 nmol/L nontargeting miRNA, miR-221, miR-494, or miR-494 inhibitor. KIT protein expression was reduced to approximately 57% of negative control (nontargeting miRNA transfection) levels after miR-494 transfection. qRT-PCR analysis indicated that KIT mRNA levels decreased in cells transfected with miR-494 and miR-221. N.C. denotes the negative control transfected with nontargeting miRNA. % denotes the relative intensity of protein expression.

There were no remarkable differences in the efficacy of miR-221 and miR-222 in downregulating KIT (data not shown). Then, we measured miR-494 expression in 4 gastric cancer cell lines, GIST882 cells and HeLa cells to determine why miR-494 inhibition did not affect KIT expression in GIST882 cells. As expected, GIST882 cells exhibited very low miR-494 expression (less than 10% of that in the other cell lines; Supplementary Fig. S4). These results indicate that KIT expression is regulated by miR-494.

Identifying 2 seed match sites in the 3′-UTR of KIT

We confirmed that KIT mRNA is a direct target of miR-494 by identifying miR-494–binding sites in the 3′-UTR of KIT. Searching the Target Scan 3.0 database (http://www.targetscan.org/) to find algorithm-based–binding sites of miR-494 in the 3′-UTR of KIT mRNA, 1 binding site was predicted at nucleotide positions 1,897 to 1,903 (site 3; Fig. 2A). We first generated the N vector, which contained the coding sequences for *Renilla* luciferase and the entire wild-type 3′-UTR sequences of the KIT mRNA. Then, we conducted a reporter assay in which 5 nmol/L nontargeting miRNA, miR-494, miR-221, or miR-222 was transfected with the N, O, or M into HeLa and SNU216 cells. Similar results were obtained in both cell lines and the figure shows representative data from HeLa cells. To confirm the induced expression of exogenous miR-494, we extracted RNA from separately collected small amounts of cells used for the DLR assay. Compared with that of the negative control, an approximate 10-fold increase in miR-494 expression was observed in HeLa cells transfected with 5 nmol/L miR-494 (Supplementary Fig. S3B). The reporter assay revealed that cells transfected with the N vector and miR-494 exhibited approximately half of the luciferase activity compared with cells transfected with the N vector and nontargeting miRNA and more severe decreases in luciferase activity than cells transfected with miR-221 and miR-222. The results also showed that the luciferase activity in cells transfected with the O vector and miR-221 or miR-222 was fully recovered compared with that in the negative control (cells transfected with the N vector and nontargeting miRNA), indicating that miR-221 and miR-222 directly target KIT mRNA. However, samples transfected with the M vector and miR-494 only had slightly recovered luciferase activity compared with that of the negative control (Fig. 2B). On the basis of this result, we hypothesized that (i) miR-494 may not directly target the 3′-UTR of KIT or (ii) additional miR-494–binding sites may exist.

We manually searched for additional potential miR-494–binding sites with Vector NTI software (Invitrogen; Fig. 2A). The 3′-UTR of KIT had 3 additional putative miR-494–binding sites that harbor 6 to 7 seed match sequences with miR-494. The putative miR-494–binding sites were TGTTTC (site 1, nucleotide positions 1,222–1,227), GTGTTTC (site 2, 1,758–1,764), and ATGTTT (site 4, 1,918–1,923; Fig. 3A). These findings led us to create 3 additional vectors, Ma, Mb, and Mc, which were derived from the M vector by additional mutagenesis (GTTT → CCGG) of the potential miR-494–binding sites. The reporter assay was conducted by transfecting the M, Ma, Mb, or Mc vector with miR-494 into HeLa and SNU216 cells. Only the cells transfected with Mb and miR-494 had fully recovered luciferase activity compared with that in the negative control (Fig. 2C). Because the G (1753) of the GTGTTTCT sequence (1,753–1,760) can hydrogen bond with U via a wobble match, this site worked nearly and the same original-binding site suggested by Target Scan 3.0. We also found that only the Mb vector fully restored luciferase activity in GIST882 cells when it was cotransfected with miR-494 (Supplementary Fig. S5). On the basis of these results we concluded that 2 different sites are important for miR-494 to bind the 3′-UTR of KIT.

Restoring KIT expression after miR-494 inhibition in the cell lines with high miR-494 expression

We determined the ability of endogenous miR-494 to bind to the 3′-UTR of KIT by designing a reporter assay using the N vector and an miR-494 inhibitor. Prior to this

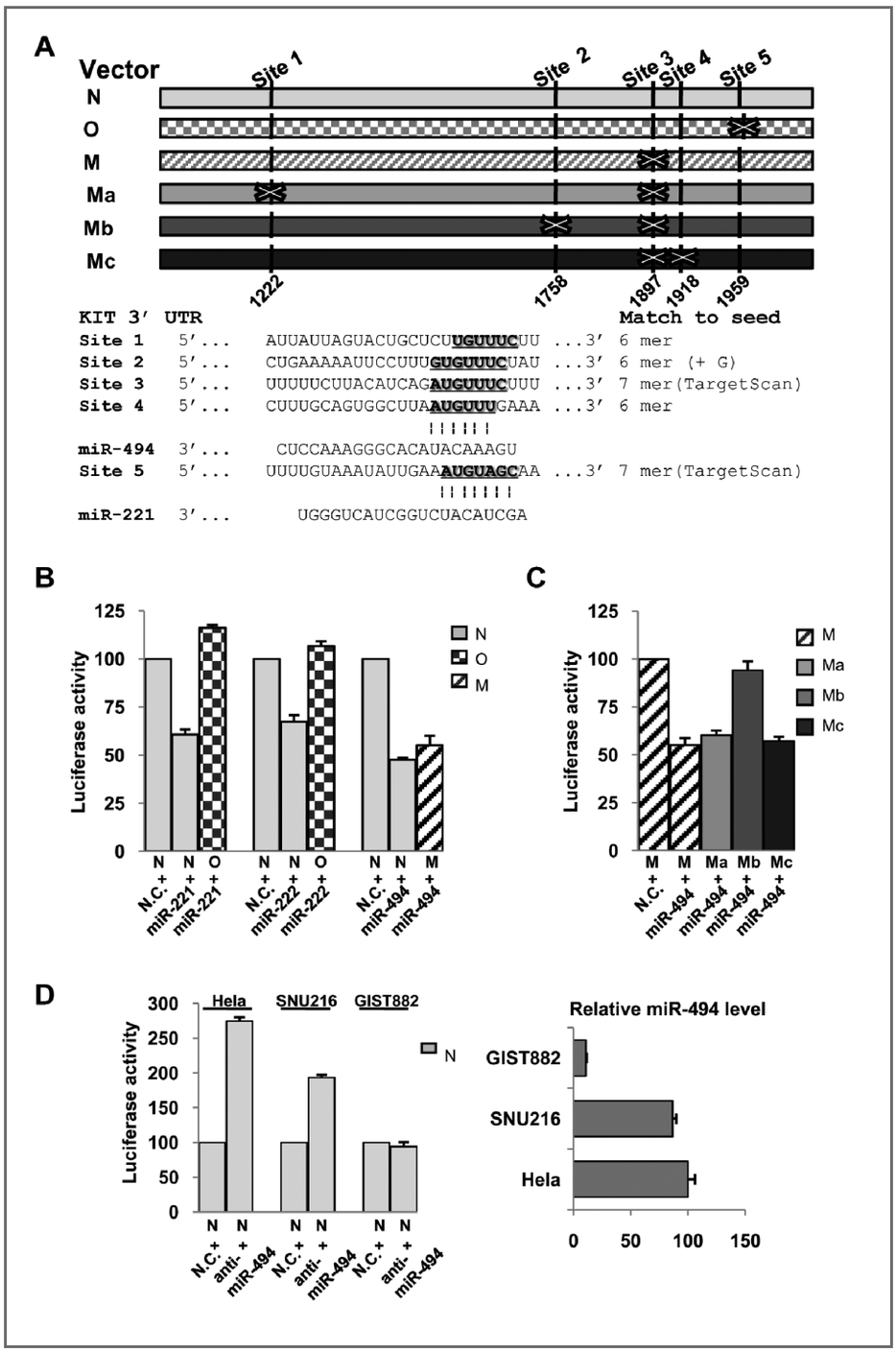

Figure 2. Identification of 2 binding sites for miR-494 in the KIT 3′-UTR. A, schematic diagram of vector constructs used in the reporter assay. The N vector contained the coding sequences for *Renilla* luciferase and the entire 3′-UTR sequence of KIT. The M construct included 4 mutated nucleotides (GTTT → CCGG) from the TargetScan3.0 expected binding seed sequences for miR-494. The Ma, Mb, and Mc constructs were generated from the M construct by substituting 4 nucleotides (every GTTT → CCGG) in putative miR-494–binding sites. The O vector was generated from N vector by substituting site 5 (GTAG → CAGA) to confirm that all constructs worked properly by showing the proper targeting of miR-221/miR-222 to the KIT 3′-UTR. B, reporter assay for the identification of seed match sites. HeLa cells were transfected with either the M construct and miR-494 or the O construct and miR-221. Luciferase activity was rescued when the O vector was cotransfected with miR-221 or miR-222. Transfection of miR-494 and the M mutant vector resulted in only slight restoration, suggesting the site 3 is not the only effective seed match site. C, reporter assay for the identification of additional binding sites. The Mb construct, which included additional mutated nucleotides in site 2 (positions 1,760–1,763) and was transfected together with miR-494, fully rescued the luciferase activity compared with that in the sample transfected with the M construct. These results indicate that site 2 is another effective seed match site for miR-494. D, restoring KIT expression after miR-494 inhibition in cells with high miR-494 expression. The N vector and miR-494 inhibitor were cotransfected into HeLa, SNU216, and GIST882 cells. HeLa and SNU216 cells, which exhibit high miR-494 expression, exhibited restored KIT expression after miR-494 inhibition. N.C. denotes the negative control transfected with nontargeting miRNA.

inhibition assay, we selected 3 cell lines (HeLa, SNU216, and GIST882) based on their endogenous miR-494 expression levels. HeLa and SNU216 cells had relatively high miR-494 expression, but miR-494 expression was barely detectable in GIST882 cells. These 3 cell lines were each transfected with the N vector and nontargeting miRNA (for negative control) or with the N vector and an miR-494 inhibitor. The cells were harvested after 2 days, and the DLR assay was carried out. SNU216 and HeLa cells transfected with an miR-494 inhibitor had approximately 2-fold higher luciferase activities than their respective negative controls. As expected, no changes in luciferase activity were observed in GIST882 cells because these cells express very low levels of miR-494 (Fig. 2D). These results indicate that KIT

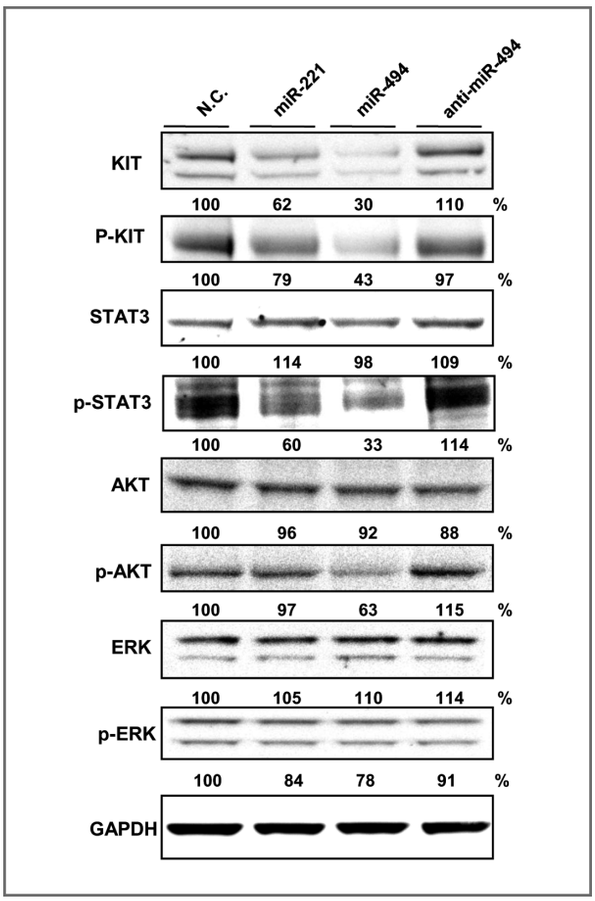

Figure 3. Decreased expression of p-AKT and p-STAT3 in GIST882 cells transfected with miR-494. Transfection of miR-494 into GIST882 cells induced significant changes in the AKT and STAT signaling pathways. The expression levels of KIT and phospho-KIT were markedly reduced after transfecting GIST882 cells with miR-494. The expression of both phospho-AKT and phospho-STAT3, downstream molecules of KIT signaling pathways, was decreased. Little difference was found between control samples and those treated with the miR-494 inhibitor. % denotes the relative intensity of protein expression. N.C. denotes the negative control transfected with nontargeting miRNA.

expression is directly regulated by endogenous miR-494 even in cell lines that do not express KIT, such as HeLa and SNU216 cells. We also carried out a reporter assay to determine whether the M or Mb vector is affected by miR-494 inhibition. As expected, whereas the M vector was affected by both miR-494 overexpression and miR-494 inhibition, the Mb vector was not affected by either condition. These results confirmed that 2 different binding sites are important for binding between miR-494 and the KIT 3′-UTR. Both M and Mb vectors were affected by miR-221 overexpression, thus indicating that the constructs worked properly (Supplementary Fig. S6).

Signaling perturbed after miR-494 treatment

The KIT downstream molecular pathway is known to be related to cell proliferation, differentiation, and apoptosis. The regulation of KIT expression affects critical pathways including AKT, ERK, and JACK-STAT pathways, as suggested by many studies (6). The effects of miR-494 on those pathways were shown by analyzing the status of p-AKT, p-ERK, p-KIT, and p-STAT3 after miR-494 transfection. GIST882 cells were transfected with 50 nmol/L nontargeting miRNA, miR-494, miR-221, or an miR-494 inhibitor. Transfection with miR-494 significantly reduced KIT expression in these cells. Transfection with miR-221 also reduced KIT expression but to a lesser extent than miR-494 transfection. As expected, miR-494 inhibition did not influence KIT expression due to the very low endogenous miR-494 expression level in the GIST882 cell line. Expression of phospho-KIT (pY703) was examined with a phospho-specific antibody and found to significantly decrease in cells transfected with miR-494. The active forms of the 3 downstream molecules in KIT signaling pathways, AKT, ERK, and STAT3, were then analyzed. The expression of phospho-AKT, as measured by a phospho-AKT–specific antibody, was decreased by miR-221 and miR-494 overexpression, with the downregulation of phospho-AKT being much larger after miR-494 overexpression than after miR-221 overexpression. The pattern of changes in phospho-STAT3 expression was similar to that of phospho-AKT expression after miR-221 and miR-494 overexpression and the decreases were larger after miR-494 overexpression. No significant change in phospho-ERK expression was observed (Fig. 3).

Induced miR-494 overexpression inhibits GIST cell proliferation

The effect of miR-494 on the proliferation of GIST882 cells was determined by a cell proliferation assay. During the assay, the normalcy of cell morphology was regularly confirmed. No remarkable changes occurred after 3 days. However, the cells transfected with miR-494 had markedly reduced numbers of cells and cell clusters 6 days after the first transfection, and these changes became more severe on the 12th day of the assay. Whereas GIST882 cells normally exhibit a spindle shape with pin-point end structure, GIST882 cells transfected with miR-494 had altered cell morphology on the 12th day of the assay (Fig. 4A), and their cell numbers were reduced to approximately 37% of the number of control group cells (Fig. 4B). In addition, we found increased numbers of dead cells floating in the culture media after miR-494 transfection. Sustained KIT downregulation was confirmed by Western blotting of the same samples used in a proliferation assay (Fig. 4C).

We used another cell model to verify the biological effects of miR-494 that is not cell line specific and common to the other cells with activated KIT. Wild-type KIT is activated by stem cell factor (SCF), whereas mutant KIT is constantly activated without SCF (6, 22). We selected DLD-1, which overexpresses wild-type KIT, to validate the effect of miR-494 treatment. By using this SCF–KIT signaling model, we tried to confirm the biological effects of miR-494 on the cells with activated KIT (23). We showed that DLD-1 cell line overexpresses KIT by RT-PCR and Western blotting

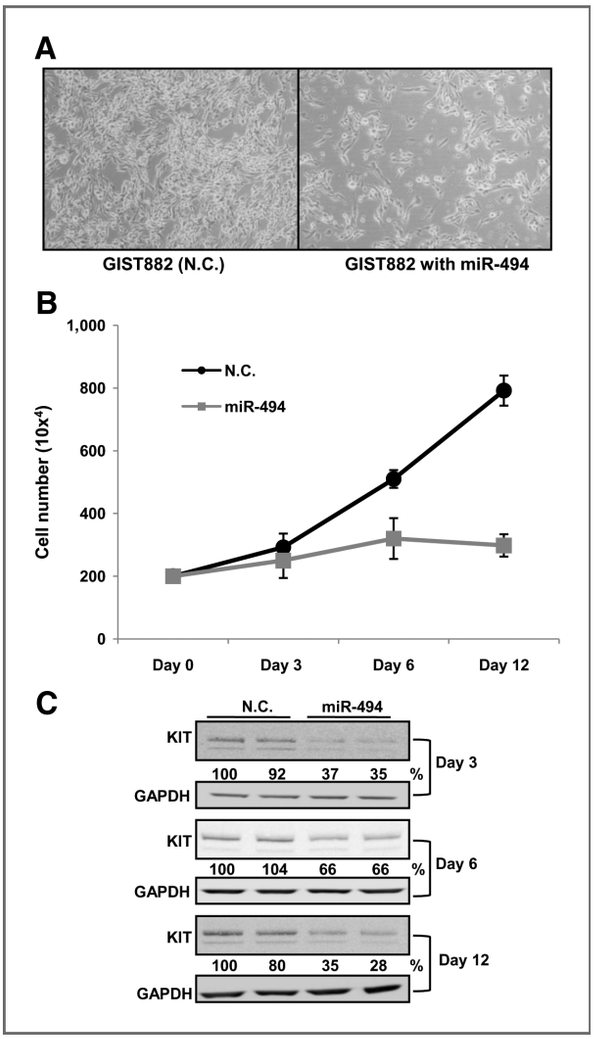

Figure 4. GIST cell proliferation is inhibited by miR-494. A, the morphology of GIST882 cells is shown 12 days after transfection. GIST882 cells transfected with miR-494 had sparse cell clusters and irregular cell morphology on the 12th day. B, the number of GIST882 cells treated with miR-494. GIST882 cells exhibited markedly reduced numbers of cells and cell clusters 6 days after the first transfection, and these changes became more severe on the 12th day of the assay. C, Western blots of the samples in the proliferation assay revealed that the GIST882 cells transfected with miR-494 had reduced KIT expression. % denotes the relative intensity of protein expression. N.C. denotes the negative control transfected with nontargeting miRNA.

(Supplementary Fig. S7A). In DLD-1 cell line, the level of p-AKT and the level of p-ERK were not detectable before SCF stimulation. SCF stimulation in the DLD-1 cell line induces large amounts of both p-KIT, p-AKT and a small amount of p-ERK. On the basis of these results, we firstly showed that miR-494 transfection reduces the KIT protein expression to approximately 40% of the expression of the negative control at both mRNA and protein levels (Supplementary Fig. S7B). When the DLD-1 cell line stimulated with SCF was treated with miR-494, the levels of p-KIT, p-AKT, and p-ERK were markedly decreased (Supplementary Fig. S7C). Also, the enhanced cellular proliferation of the DLD-1 cell line with SCF treatment was markedly inhibited after miR-494 treatment (Supplementary Fig. S7D).

Apoptosis and cell-cycle analysis after miR-494 overexpression in GIST882 cells

Changes in the cell-cycle distribution of GIST882 cells after miR-494 transfection was assessed by flow cytometry. Cells transfected with miR-494 had a 6% increase in the number of G_0–G_1 phase cells and a 5% decrease in the number of S phase cells compared with cells transfected with nontargeting miRNA (Fig 5A). These findings indicate that miR-494 inhibits GIST882 cell proliferation by modulating the cell cycle. We also examined apoptotic changes after miR-494 transfection by using a combination of Annexin V and PI. The result indicated that approximately 25% of cell populations undergo early or late apoptotic changes after miR-494 transfection (Fig 5B). Reduced KIT expression was confirmed by Western blotting during the experiment. These data indicate that miR-494 treatment induces both cell-cycle arrest and apoptosis in GIST882 cells.

Discussion

miRNAs can posttranscriptionally regulate target genes and components of target gene regulatory pathways, thus affecting signal transduction both directly and indirectly. These findings suggest that miRNAs play major regulatory roles in signal transduction pathways and tumorigenesis (15, 16). Mutations of *KIT* and KIT overexpression are interrelated with KIT-induced tumorigenesis, and dysregulated miRNA expression might explain KIT overexpression and the resulting tumorigenesis (12, 13). MiR-221 and miR-222 have been reported to negatively regulate erythroleukemic cell growth by targeting KIT (17). However, no miRNAs involved in GIST tumorigenesis by targeting KIT have been reported. We herein proposed that miR-494 directly targets KIT by showing that exogenous miR-494 induces KIT downregulation, and miR-494 inhibition induces KIT overexpression. Downregulation of KIT occurs more potently *in vitro* with miR-494 than with miR-221 and miR-222, the previously reported KIT-targeting miRNAs. Moreover, the expression level of miR-221 and miR-222 was not related to KIT expression in GISTs (13).

Until now, the role of miR-494 in GISTs and other diseases was poorly understood. No genes had been reported to be targeted by miR-494, excluding a report that miR-494 could downregulate PTEN expression in a chemically transformed cell line (24). However, we could not show significant changes in PTEN expression after miR-494 overexpression in GIST882 cells (Supplementary Fig. S8). Other studies reported the decreased expression of miR-494 in lymphoma and squamous cell carcinoma of the head and neck in miRNA microarray profiling studies (25, 26); however, the direct relationship between this decreased expression and tumor-related gene expression has not been

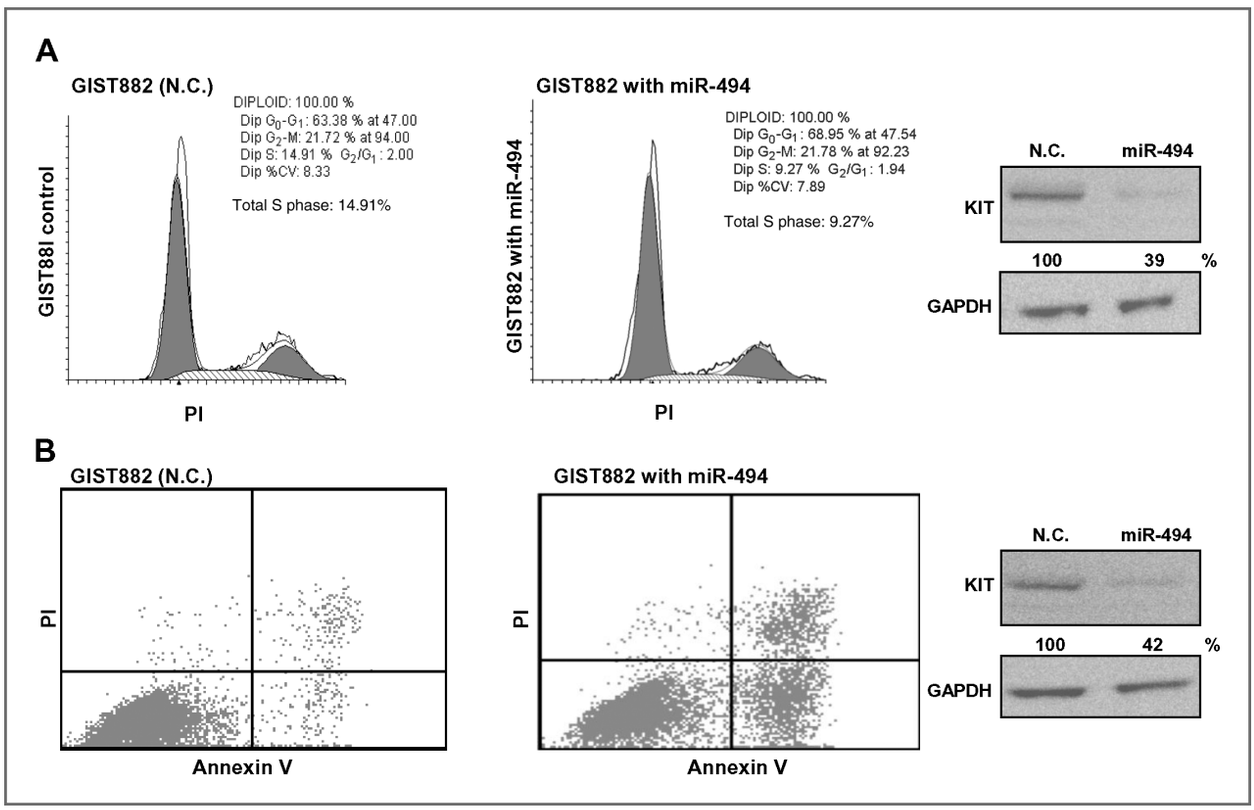

Figure 5. Analysis of apoptosis and cell-cycle distribution after miR-494 transfection. A, cell-cycle analysis after miR-494 transfection. GIST882 cells transfected with nontargeting miRNA (left) or miR-494 (right) were harvested on day 4 and stained with PI. miR-494 transfection resulted in a 5.6% increase in the number of G_0–G_1 phase cells and a 5.7% decrease in the number of S phase cells relative to the cell numbers for cells treated with nontargeting miRNA. B, apoptosis analysis after miR-494 transfection. Six days after transfection with or without miR-494, GIST882 cells were stained with PI and Annexin V. Approximately 25% of GIST882 cells treated with miR-494 undergo apoptosis. % denotes the relative intensity of protein expression. N.C. denotes the negative control transfected with nontargeting miRNA.

reported. In addition to the inverse expression between KIT and miR-494 expression in GISTs, we showed that miR-494 directly downregulates KIT by binding 2 different seed match sites. We also showed miR-494 inhibition induces KIT overexpression. Therefore, we conclude that miR-494 is a major miRNA that regulates KIT in GISTs.

The protein KIT is a highly oncogeneic tyrosine kinase that belongs to the RTK family and is involved in the major signal transduction pathways of PI3 kinase-AKT, Src family kinase, and Ras-ERK and in the minor signal transduction pathway of JAK-STAT. Wild-type KIT is activated by SCF, whereas mutant KIT is constantly activated without SCF (6, 22, 23). Mutations of the transmembrane domain constantly activate KIT receptor dimerization, leading to the activation of downstream signaling (27). Gain-of-function mutations are frequently found in exons 9, 11, 13, and 17 of the KIT gene and contribute to GIST tumorigenesis (3, 28). This study showed that the downregulation of mutant KIT induced by miR-494 affects the expression of p-AKT and p-STAT3. These findings are consistent with previous reports indicating that p-AKT and p-STAT3 expression were decreased after GIST882 cells with activated KIT were treated with imatinib or KIT short hairpin RNA. Moreover, we also showed that the induced p-AKT and p-ERK by SCF stimulation in the wild-type KIT overexpressing cells are specifically decreased after miR-494 transfection.

Imatinib inhibits KIT through its ATP-binding pocket, affecting KIT phosphorylation and subsequently inactivating downstream molecules (29–32). Our study showed that miR-494 transfection has similar effects on GIST882 cells as imatinib, such as perturbing signaling pathways and suppressing cell proliferation. These findings indicate that miR-494 overexpression could be another alternative treatment option for GISTs. Our identification of 2 different seed match sites for miR-494 in the 3′-UTR of KIT further supports the concept of KIT mRNA as the direct target of miR-494 and creates more practical therapeutic possibilities for GISTs with KIT activation.

Oncoproteins can be inhibited posttranslationally or posttransciptionally (33). The inhibition of KIT by imatinib is an example of posttranslational inhibition through competitively binding the ATP-binding pocket of KIT. However, KIT inhibition by imatinib is imperfect because resistance can occur through putative mutations that can develop in

the specific amino acid sequences during treatment. The resultant imatinib resistance occurs through the inhibition of imatinib binding to the ATP-binding pocket of KIT (11). More therapeutic options are needed for resistance caused by these mutations. The therapeutic use of miR-494 to inactivate KIT will continue to be challenging because traditional RNA-based therapies are instable in blood and siRNAs have paradoxically large molecular sizes. However, many of these problems are being solved by new delivery systems such as aptamers, nanoparticles, and liposomes (34–36). Applying these new delivery systems will allow miR-494 to be used as a novel therapeutic tool to treat GISTs.

In conclusion, miR-494 is a potent regulator of KIT in GISTs, and introducing miR-494 into GISTs may be a novel mechanism of reversing tumor progression.

Disclosure of Potential Conflicts of Interest

No potential conflicts of interest were disclosed.

Grant Support

This research was funded by grant number FPR08A2-100 sponsored by the 21C Frontier Functional Proteomics Project, Korean Ministry of Education, Science, and Technology and by the Converging Research Center Program through the Ministry of Education, Science and Technology (2010K001115).

The costs of publication of this article were defrayed in part by the payment of page charges. This article must therefore be hereby marked *advertisement* in accordance with 18 U.S.C. Section 1734 solely to indicate this fact.

Received January 19, 2011; revised September 23, 2011; accepted October 20, 2011; published OnlineFirst October 31, 2011.

References

1. Fletcher CD, Berman JJ, Corless C, Gorstein F, Lasota J, Longley BJ, et al. Diagnosis of gastrointestinal stromal tumors: A consensus approach. Hum Pathol 2002;33:459–65.
2. Miettinen M, Lasota J. Gastrointestinal stromal tumors–definition, clinical, histological, immunohistochemical, and molecular genetic features and differential diagnosis. Virchows Arch 2001;438:1–12.
3. Miettinen M, Lasota J. Gastrointestinal stromal tumors: review on morphology, molecular pathology, prognosis, and differential diagnosis. Arch Pathol Lab Med 2006;130:1466–78.
4. Duensing A, Medeiros F, McConarty B, Joseph NE, Panigrahy D, Singer S, et al. Mechanisms of oncogenic KIT signal transduction in primary gastrointestinal stromal tumors (GISTs). Oncogene 2004;23:3999–4006.
5. Heinrich MC, Corless CL, Duensing A, McGreevey L, Chen CJ, Joseph N, et al. PDGFRA activating mutations in gastrointestinal stromal tumors. Science 2003;299:708–10.
6. Lennartsson J, Ronnstrand L. The stem cell factor receptor/c-Kit as a drug target in cancer. Curr Cancer Drug Targets 2006;6:65–75.
7. Tuveson DA, Willis NA, Jacks T, Griffin JD, Singer S, Fletcher CD, et al. STI571 inactivation of the gastrointestinal stromal tumor c-KIT oncoprotein: biological and clinical implications. Oncogene 2001;20:5054–8.
8. Gordon PM, Fisher DE. Role for the proapoptotic factor BIM in mediating imatinib-induced apoptosis in a c-KIT-dependent gastrointestinal stromal tumor cell line. J Biol Chem;285:14109–14.
9. Bauer S, Duensing A, Demetri GD, Fletcher JA. KIT oncogenic signaling mechanisms in imatinib-resistant gastrointestinal stromal tumor: PI3-kinase/AKT is a crucial survival pathway. Oncogene 2007;26:7560–8.
10. Ma Y, Zeng S, Metcalfe DD, Akin C, Dimitrijevic S, Butterfield JH, et al. The c-KIT mutation causing human mastocytosis is resistant to STI571 and other KIT kinase inhibitors; kinases with enzymatic site mutations show different inhibitor sensitivity profiles than wild-type kinases and those with regulatory-type mutations. Blood 2002;99:1741–4.
11. McLean SR, Gana-Weisz M, Hartzoulakis B, Frow R, Whelan J, Selwood D, et al. Imatinib binding and cKIT inhibition is abrogated by the cKIT kinase domain I missense mutation Val654Ala. Mol Cancer Ther 2005;4:2008–15.
12. Kang HJ, Nam SW, Kim H, Rhee H, Kim NG, Hyung WJ, et al. Correlation of KIT and platelet-derived growth factor receptor alpha mutations with gene activation and expression profiles in gastrointestinal stromal tumors. Oncogene 2005;24:1066–74.
13. Choi HJ, Lee H, Kim H, Kwon JE, Kang HJ, You KT, et al. MicroRNA expression profile of gastrointestinal stromal tumors is distinguished by 14q loss and anatomic site. Int J Cancer;126:1640–50.
14. Quek R, George S. Gastrointestinal stromal tumor: a clinical overview. Hematol Oncol Clin North Am 2009;23:69–78, viii.
15. Schickel R, Boyerinas B, Park SM, Peter ME. MicroRNAs: key players in the immune system, differentiation, tumorigenesis and cell death. Oncogene 2008;27:5959–74.
16. Calin GA, Croce CM. MicroRNA signatures in human cancers. Nat Rev Cancer 2006;6:857–66.
17. Felli N, Fontana L, Pelosi E, Botta R, Bonci D, Facchiano F, et al. MicroRNAs 221 and 222 inhibit normal erythropoiesis and erythroleukemic cell growth via kit receptor down-modulation. Proc Natl Acad Sci U S A 2005;102:18081–6.
18. Kang HJ, Koh KH, Yang E, You KT, Kim HJ, Paik YK, et al. Differentially expressed proteins in gastrointestinal stromal tumors with KIT and PDGFRA mutations. Proteomics 2006;6:1151–7.
19. Kim NG, Kim JJ, Ahn JY, Seong CM, Noh SH, Kim CB, et al. Putative chromosomal deletions on 9P, 9Q and 22Q occur preferentially in malignant gastrointestinal stromal tumors. Int J Cancer 2000;85:633–8.
20. Agaimy A. Gastrointestinal stromal tumors (GIST) from risk stratification systems to the new TNM proposal: more questions than answers? A review emphasizing the need for a standardized GIST reporting. Int J Clin Exp Pathol 2010;3:461–71.
21. Livak KJ, Schmittgen TD. Analysis of relative gene expression data using real-time quantitative PCR and the 2(-Delta Delta C(T)) Method. Methods 2001;25:402–8.
22. Bellone G, Carbone A, Sibona N, Bosco O, Tibaudi D, Smirne C, et al. Aberrant activation of c-kit protects colon carcinoma cells against apoptosis and enhances their invasive potential. Cancer Res 2001;61:2200–6.
23. Yasuda A, Sawai H, Takahashi H, Ochi N, Matsuo Y, Funahashi H, et al. Stem cell factor/c-kit receptor signaling enhances the proliferation and invasion of colorectal cancer cells through the PI3K/Akt pathway. Dig Dis Sci 2007;52:2292–300.
24. Liu L, Jiang Y, Zhang H, Greenlee AR, Han Z. Overexpressed miR-494 down-regulates PTEN gene expression in cells transformed by anti-benzo(a)pyrene-trans-7,8-dihydrodiol-9,10-epoxide. Life Sci 2010;86:192–8.
25. Chang SS, Jiang WW, Smith I, Poeta LM, Begum S, Glazer C, et al. MicroRNA alterations in head and neck squamous cell carcinoma. Int J Cancer 2008;123:2791–7.
26. Robertus JL, Kluiver J, Weggemans C, Harms G, Reijmers RM, Swart Y , et al. MiRNA profiling in B non-Hodgkin lymphoma: a MYC-related miRNA profile characterizes Burkitt lymphoma. Br J Haematol 2010;149:896–9.
27. Lux ML, Rubin BP, Biase TL, Chen CJ, Maclure T, Demetri G, et al. KIT extracellular and kinase domain mutations in gastrointestinal stromal tumors. Am J Pathol 2000;156:791–5.
28. Nakahara M, Isozaki K, Hirota S, Miyagawa J, Hase-Sawada N, Taniguchi M, et al. A novel gain-of-function mutation of c-kit gene in gastrointestinal stromal tumors. Gastroenterology 1998;115:1090–5.

29. Demetri GD. Structural reengineering of imatinib to decrease cardiac risk in cancer therapy. J Clin Invest 2007;117:3650–3.
30. Heinrich MC, Griffith DJ, Druker BJ, Wait CL, Ott KA, Zigler AJ. Inhibition of c-kit receptor tyrosine kinase activity by STI 571, a selective tyrosine kinase inhibitor. Blood 2000;96:925–32.
31. Joensuu H, Roberts PJ, Sarlomo-Rikala M, Andersson LC, Tervahartiala P, Tuveson D, et al. Effect of the tyrosine kinase inhibitor STI571 in a patient with a metastatic gastrointestinal stromal tumor. N Engl J Med 2001;344:1052–6.
32. Ou WB, Zhu MJ, Demetri GD, Fletcher CD, Fletcher JA. Protein kinase C-theta regulates KIT expression and proliferation in gastrointestinal stromal tumors. Oncogene 2008;27:5624–34.
33. Yang Y, Zhou F, Fang Z, Wang L, Li Z, Sun L, et al. Post-transcriptional and post-translational regulation of PTEN by transforming growth factor-beta1. J Cell Biochem 2009;106:1102–12.
34. Semple SC, Akinc A, Chen J, Sandhu AP, Mui BL, Cho CK, et al. Rational design of cationic lipids for siRNA delivery. Nat Biotechnol 2010;28:172–6.
35. Pastor F, Kolonias D, Giangrande PH, Gilboa E. Induction of tumour immunity by targeted inhibition of nonsense-mediated mRNA decay. Nature 2010;465:227–30.
36. Wang T, Li M, Gao H, Wu Y. Nanoparticle carriers based on copolymers of poly(epsilon-caprolactone) and hyperbranched polymers for drug delivery. J Colloid Interface Sci 2011;353:107–15.